THE UNIVERSITY *of* EDINBURGH

Edinburgh Research Explorer

Thermal integration of Waste to energy plants with Post-combustion CO2 capture

OPEN ACCESS
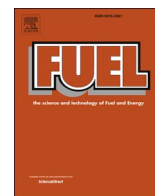
Thermal integration of waste to energy plants with Post-combustion CO₂ capture

Dan Su [a], Laura Herraiz [a], Mathieu Lucquiaud [b], Camilla Thomson [a], Hannah Chalmers [a],[*]

[a] School of Engineering, University of Edinburgh, Edinburgh, UK
[b] Department of Mechanical Engineering, University of Sheffield, Sheffield, UK

ARTICLE INFO

ABSTRACT

Waste-to-Energy (WtE) is becoming an important application sector for carbon capture utilization and storage (CCS) due to its role in urban waste management and its inherent potential of achieving negative emissions. This study is built upon a series of modelling activities, with three representative WtE plant steam cycle configurations selected to integrate monoethanolamine (MEA) based Post-combustion CO₂ Capture (PCC). With 60% biogenic carbon in the fuel, a set of key performance indicators of the investigated WtE plant configurations are presented. Results show that there is significant potential for heat recovery from the PCC process to provide heat for District Heating (DH). With advanced heat recovery, the energy utility factor (EUF) of WtE plant could be higher than that for WtE plant without PCC. Results also show that optimised process design can be used to enable ultra-high CO₂ capture (99.72% in this study) to be achieved with only a marginal increase in specific reboiler duty when compared with 95% capture. This study also highlights the importance of differentiating carbon intensities for different product bases: electrical or thermal or waste, which are important when comparing WtE CCS with other carbon saving technologies. The findings of this study provide valuable information for the future implementation of carbon dioxide capture technology in the WtE sector.

1. Introduction

Bio-Energy with Carbon Capture and Storage (BECCS) is a promising carbon removal approach that has the potential to offer permanent net removal of carbon dioxide (CO₂) from the atmosphere over its lifetime [38]. A significant bioenergy resource is organic waste contained in municipal solid waste (MSW) that can be combusted in Waste to Energy (WtE) facilities to produce energy. Due to the high biogenic content in MSW, typically within a range from 50 % to 70 % [14,24], the adoption of Carbon Capture and Storage (CCS) in the WtE sector can play a promising role in the sustainable development of urban waste management strategies, and in delivering 'negative carbon emissions' for climate change mitigation.

Solvent-based post-combustion carbon capture (PCC) is one of several options for removing CO₂ from exhaust flue gases in power plants. It has been proposed for WtE plants since it is the most proven technology for CO₂ capture and no significant modifications to the original plant are required [1,47]. Integration of PCC in WtE facilities, however, requires a large quantity of steam extraction from the power cycle for solvent regeneration, which causes an energy penalty to the

WtE plant [3]. This is even more challenging for Combined Heat and Power (CHP) WtE plants with District Heating (DH) supply obligations.

In Europe, the WtE sector provides up to 15 % of existing DH demand and the trend is increasing [7,46]. Reports from two surveys of European WtE plants show that around 50 % operate as CHP plants [35,40]. In northern countries with cool climatic conditions, such as Denmark and Sweden, it has become common practice to use heat from WtE plants for public heating purposes. In eastern and central Europe, WtE plants with DH systems also exist and are attracting more interest due to the relatively high system efficiency and low CO₂ emissions when compared with power only plants [10,27,30,42].

It is vital for CHP WtE plants with PCC to investigate approaches to balance the heat supply for the CO₂ capture process and for the DH network, and thus design options for an effective thermal integration. Previous studies indicate that heat recovery is technologically viable to tackle the 'energy conflict' and to achieve more effective integration [15,23,48]. Improved heat exchanger network synthesis is proposed by Yoro et al. to tackle the high energy and material requirement of CO₂ separation process [45].

The application of CCS in the WtE sector is an emerging field that has

---

* Corresponding author.
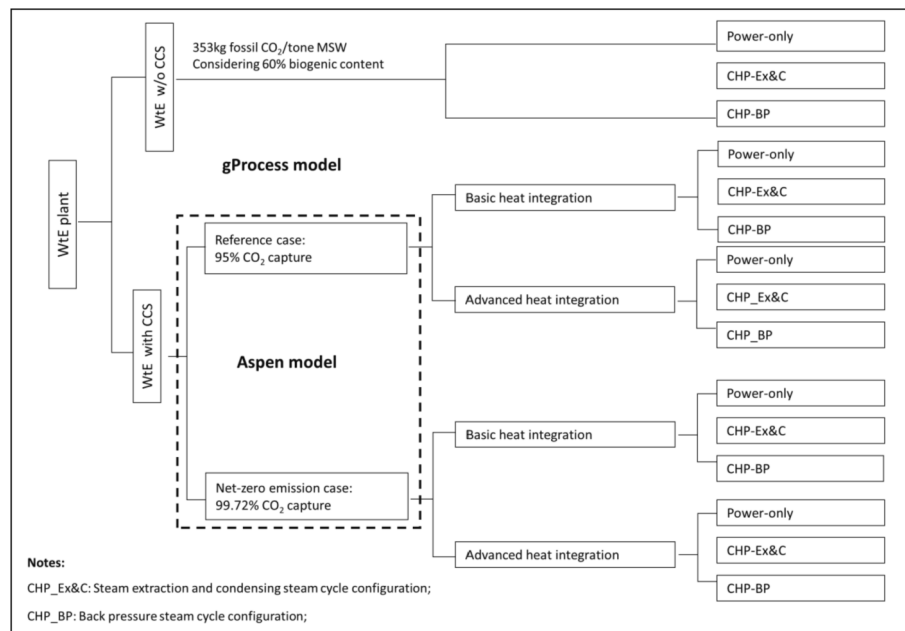 E-mail address: hannah.chalmers@ed.ac.uk (H. Chalmers).

Fig. 1. Investigated process modelling approaches.

been getting more attention in recent years, and a limited number of studies have been published [16,29,39]. The world's first full-scale commercial WtE with CCS plant, Hafslund Oslo Celsio - Klemetsrud CCS Project, secured full financing in 2022 and is expected to capture 400kt CO_2/yr from 2025 [26,34].

Another consideration for the integration of PCC with WtE plant is that 'Net-zero' is changing the expectation of residual emissions from CCS; in particular, ultra-high capture levels (>99 %) have been proposed. Recent studies show that >99 % capture levels are technically feasible and the additional CO_2 capture increases costs within an acceptable range [9,18,20,25]. Recent guidelines published by the UK Environmental Agency for permitting new post-combustion CO_2 capture plants for gas and biomass power plants require a design CO_2 capture rate of at least 95 % to be achieved for an environmental permit to be approved [13]. It is necessary to assess the technical and operational implications of ultra-high CO_2 levels in WtE facilities equipped with PCC, in terms of the system performance and the negative carbon emission potentials.

In this work, a rigorous model of a WtE plant equipped with an amine-based CO_2 capture and compression system is developed with the focus of the following objectives:

1) Identify how to optimise the process through CO_2 capture process modelling for different capture rates;
2) Calculate the excess heat recoverable from the capture plant that may be available for DH supply;
3) Identify what the key indicators are that can be used to evaluate the performance of the thermal integration;
4) Determine how to present the carbon emission intensity of different types of WtE with CCS accurately, paying particular attention to the range of products delivered by the plant.

This work provides valuable insights on the performance of a WtE plant with PCC connected to electricity and district heat networks, and recommendations for future deployment of CO_2 capture technologies in the WtE sector.

2. Methodology

In order to assess the performance of a WtE facility equipped with

post-combustion CO_2 capture and compression, a generic medium size WtE plant using direct combustion over a moving grate is modelled, with a constant 500 t/d MSW consumption (55MWth thermal energy input). As described in Section 2.1, three operating scenarios are considered:

a) 'Power-only' represents WtE plants with power only operation
b) 'CHP-Ex&C' represents WtE plants with steam extraction and a condensing steam turbine
c) 'CHP-BP' represents WtE plants with a back pressure steam turbine

For each scenario, two CO_2 capture rates are considered: 95 % and 99.72 %, as described in Section 2.2.2. Additionally, two thermal integration options are considered for each CO_2 capture rate: basic and advanced, as described in Section 2.2.3. For this purpose an amine-based carbon capture system is built in ASPEN Plus V10, using a 35 %wt monoethanolamine (MEA) aqueous solution to ensure a relatively low specific reboiler duty (SRD) at high CO_2 capture efficiency [17]. This is embedded in a rigorous integration model of a WtE facility with PCC, which includes a three-stage CO_2 compression train and is built in gProcess V2.0.0. Fig. 1 summarises the process modelling approaches considered in this article.

2.1. Investigated configurations of the WtE plant without PCC

The technology most widely used for energy recovery from MSW is direct combustion over a moving grate, with the generation of super-heated steam feeding a steam turbine train for power generation [44]. Based on a collection of WtE facility data from an extensive literature review [4,6,11,27], three configurations of the WtE plant representative of the WtE facilities in operation in Europe are considered in this article:

a) In the power-only configuration, the WtE plant produces only electricity and the steam turbine train comprises a condensing steam turbine (ST) where superheated steam expands from 60 bar to a condenser pressure of 0.1 bar, considered in this work for an air cooling system. This configuration is representative of WtE plants which are not connected to a DH network including, but not limited to, plants that are built as DH ready (i.e. they will provide DH in the future) or CHP WtE plants currently connected to a DH network
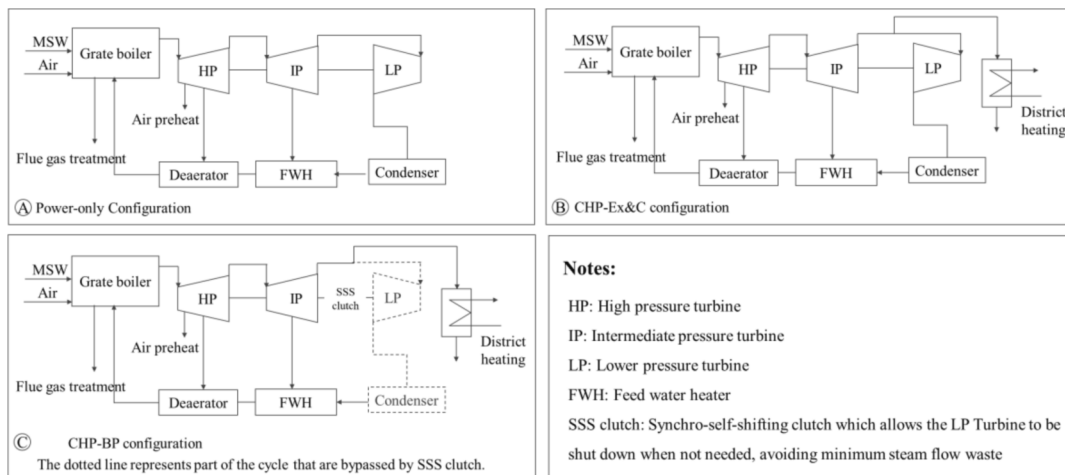
Fig. 2. Schematic representation of investigated configurations of the WtE plant.
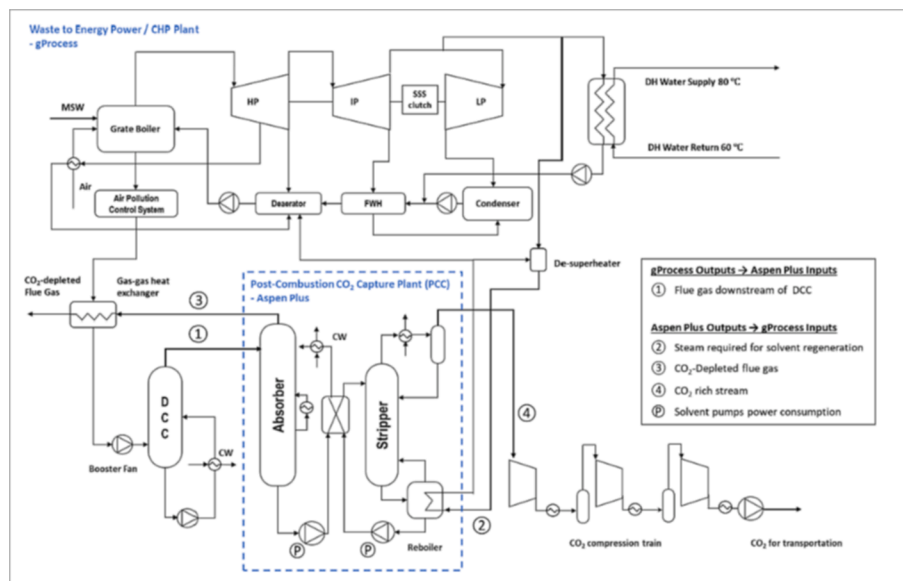

Fig. 3. Process flow diagram of a WtE CHP plant with CO_2 capture and compression.

operating during summer time when the DH demand is expected to be zero.

b) In the CHP-Ex&C configuration, the WtE plant produces electricity and thermal energy for the DH system. The steam turbine train consists of a high pressure (HP) ST cylinder and a condensing low pressure (LP) ST cylinder connected to an air-cooler condenser. Superheated steam expands from 60 bar to 4 bar in the HP steam turbine cylinder, a fraction of steam is then extracted to supply thermal energy to the DH system, and the remaining steam expands in the LP steam turbine cylinder from 4 bar to the condenser pressure (i.e. 0.1 bar). A constant steam extraction to the DH system is assumed with and without PCC and, thus, additional steam extraction for CO_2 capture will only penalise the electricity output. It is assumed that the minimum flow rate through the LP steam turbine cylinder is 15 % of the nominal flow rate at full load, to cool down the blades and avoid overheating by churning.

c) In the CHP-BP configuration, the WtE plant produces electricity and thermal energy for the DH system. The steam turbine train consists of a HP ST cylinder and a back pressure LP ST cylinder. Superheated steam expands from 60 bar to 4 bar and it is then sent to the DH system. When PCC is implemented, part of the steam is sent to the

reboiler of the CO_2 capture plant. In reality, the steam turbine train can be designed with a Synchro-Self-Shifting (SSS) clutch, which could be used to decouple the HP and the LP cylinders so that no minimum steam flow rate is required through the LP cylinder [5]. This operation scenario is representative of WtE plants with high DH demand during the whole year and particularly CHP WtE plants located in regions with long cold winters.

Fig. 2 shows a schematic representation of the three WtE plant configurations. For all three configurations, the power-only configuration is used as the base case plant. For example, the swallowing capacity of the LP steam turbine cylinder for power-only operation is also used for the other operating configurations. When PCC is on, a throttling valve located downstream of the extraction point is used to maintain the IP/LP crossover pressure at the required level.

2.2. Modelling methodology of a WtE facility with PCC

The three WtE configurations described in Section 2.1 are used as generic configurations and are equipped with a post-combustion CO_2 capture system and a CO_2 compression train developed in gProcess
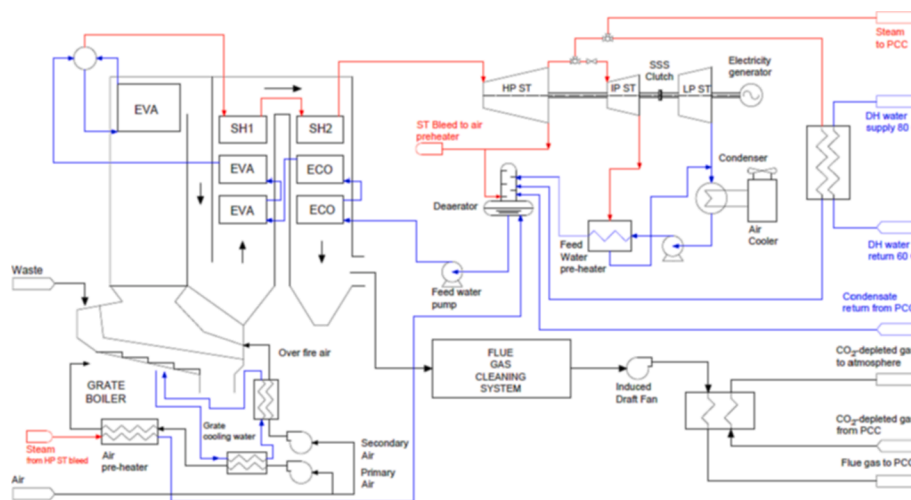
Fig. 4. Schematic layout of the referenced WtE plant.
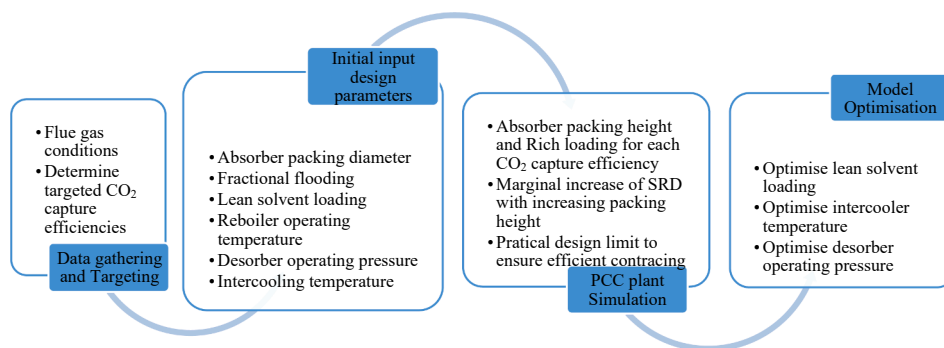
Fig. 5. PCC plant modelling approach in ASPEN plus.
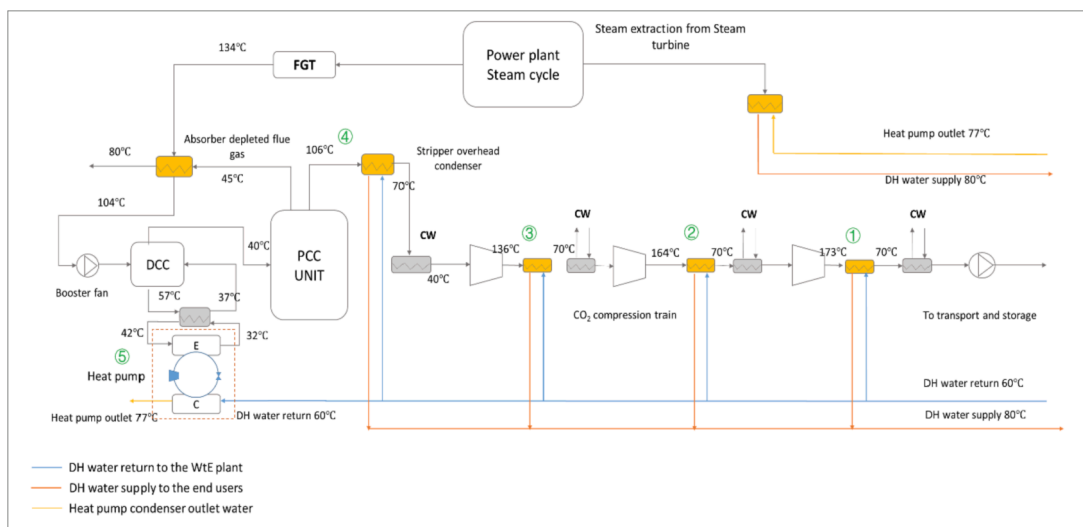
Fig. 6. Schematic representation of the additional heat recovery options considered in the advanced heat integration configuration of a CHP WtE with post-combustion CO_2 capture.

V2.0.0. gProcess is an equation-oriented modelling platform that allows the creation of customised models for each operation, using the Peng-Robinson equation of state for gas mixtures and Steam Tables (IEAPWS-95) for water and steam available in Multiflash V6.1.

The CO_2 capture plant is separately modelled in Aspen-Plus V10 with the objective of sizing the absorber column and optimising the operating

parameters to find the minimum specific reboiler duty (SRD) required to achieve a given CO_2 capture efficiency. The starting point for the CO_2 capture plant in this paper is an open-source steady-state model of a conventional solvent-based CO_2 capture plant using 35 %wt mono-ethanolamine (MEA) aqueous solution (developed by the U.S. Department of Energy's Carbon Capture Simulation Initiative at the National

Table 1
Flue gas inlet conditions of the PCC system.

Flue gas at the inlet of the absorber		Composition
Pressure	bar	1.063
Temperature	C	40
Mass flow rate	kg/s	30.71
Molar flow rate	mol/s	1046
Composition		
CO_2	%vol	11.11
H2O	%vol	6.95
N2	%vol	75.23
O_2	%vol	6.72

Carbon Capture Centre (NCCC)) [22]. This model has been validated satisfactorily with NCCC pilot plant data from the 2014 campaign [32,41].

The PCC system in gProcess is modelled as a "grey box" which requires the following input parameters obtained from the CO_2 capture model in Aspen Plus:

- CO_2 capture efficiency (or CO_2 captured flow rate);
- SRD (or mass flow rate of steam for solvent regeneration);
- the operating stripper pressure; and
- Auxiliary power consumption by the solvent pumps.

The Aspen Plus model requires as input parameters the flow rate and composition of the flue gas exiting the direct contact cooler (DCC) and the pressure and temperature of the steam extraction available from the IP/LP crossover in the steam cycle.

An overview of the process flow diagram of the WtE plant equipped with a CO_2 capture system and a three-stage CO_2 compression train connected to a DH system is provided in Fig. 3 and a more detailed process flow diagram is available in Appendix 1. With PCC, the steam

required in the CO_2 capture process for the solvent regeneration is extracted from the main steam cycle at 4 bar. The condensate return mixes with the power plant condensate as it emerges from the feed water heating (FWH) train.

2.2.1. Description of the WtE facility

The reference WtE plant is assumed to operate as base load with a contractual obligation to process 500 t/day of MSW throughput. The schematic layout of the referenced WtE plant as shown in Fig. 4. It includes air-preheating, the waste incineration furnace and grate, flue gas passes for steam generation, steam turbines for power production, a heat exchanger for heat production, and the flue gas cleaning systems.

The MSW is processed by direct combustion over a moving grate using 50 % excess air to ensure complete combustion. Combustion air is added in two stages. Primary air (ca. 70 % of the total air) is preheated to 150 °C by steam extracted from the HP turbine and supplied through the grate layer into the fuel bed. Secondary air (ca. 30 % of the total air flow) is preheated using grate cooling water up to 50 °C and supplied over the grate layer (air over fire). The excess air is calculated so that the oxygen concentration in the exhaust flue gas is within the range of 6 % vol to 9 % vol (dry basis).

The heat released from the waste incineration is used to generate superheated steam at 400 °C and 60 bar, which is sent to the steam turbine train for power generation. The steam turbine consists of three cylinders with one steam extraction point at 6 bar for the deaerator, and a subsequent steam extraction point at 4 bar to supply the district heating system and the reboiler for solvent regeneration when operating with CO_2 capture.

The flue gas exiting the heat recovery section in the boiler goes through a series of flue gas treatment processes to remove acid gases and other harmful components. Nitrogen oxide emissions are removed using a selective non-catalytic reduction process with injection of aqueous ammonia. A series of bag filters are used to reduce the particle matter concentration to the allowed emission level. After the flue gas treatment
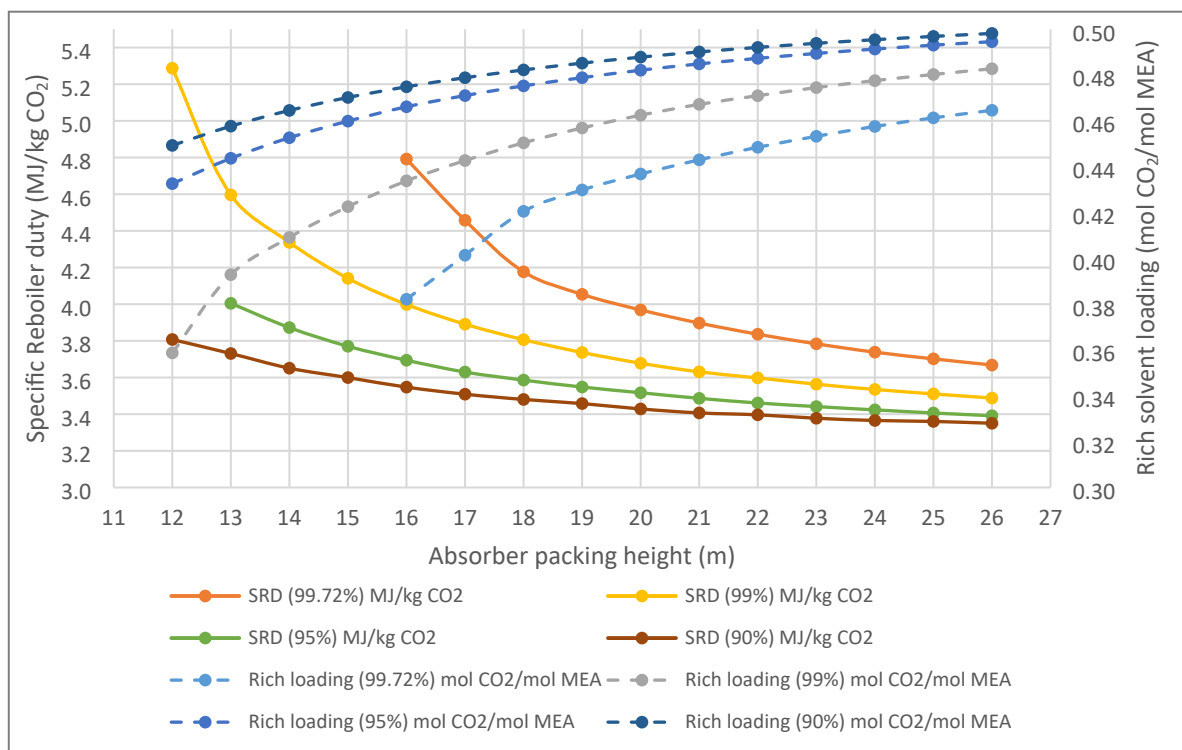

Fig. 7. Sensitivity of the absorber packing height on the rich solvent CO_2 loading (continuous line) and the specific reboiler duty (dashed lines) for a 35 %wt MEA capture system at a range of CO_2 capture rates: 90 %, 95 %, 99 % and 99.72 %.Lean loading is assumed constant at 0.16 mol CO_2/mol MEA for all the CO_2 capture rates.
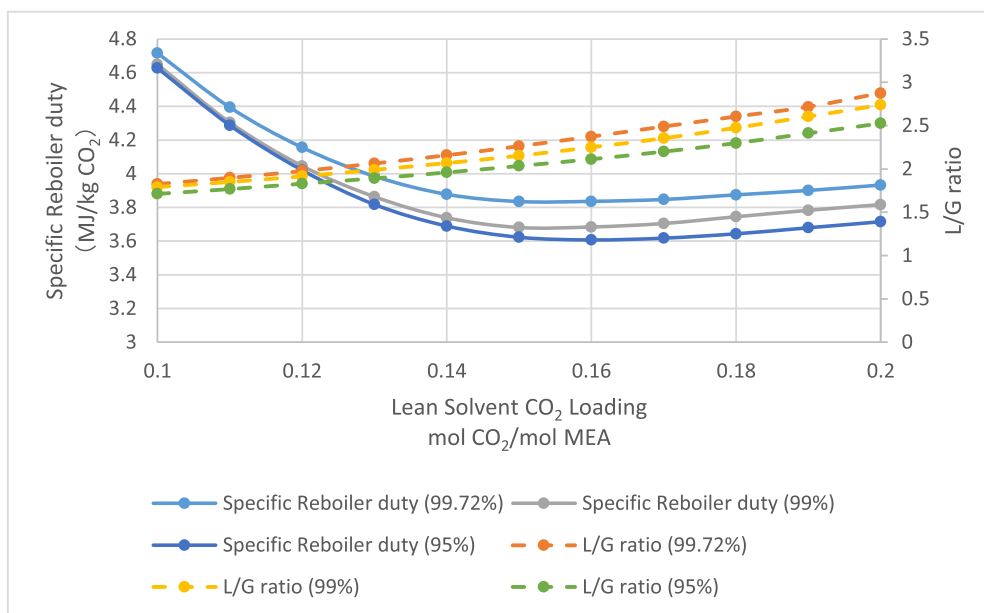
Fig. 8. Sensitivity of the specific reboiler duty to the lean solvent CO_2 loading for a 35 %wt MEA capture system for a range of CO_2 capture efficiencies 95 %/99 % /99.7 %. The absorber packing heights are 17 m/20 m/22 m for 95 %/99 % /99.7 % capture efficiencies, respectively. For illustration purposes, the final packing height after optimisation might be different.
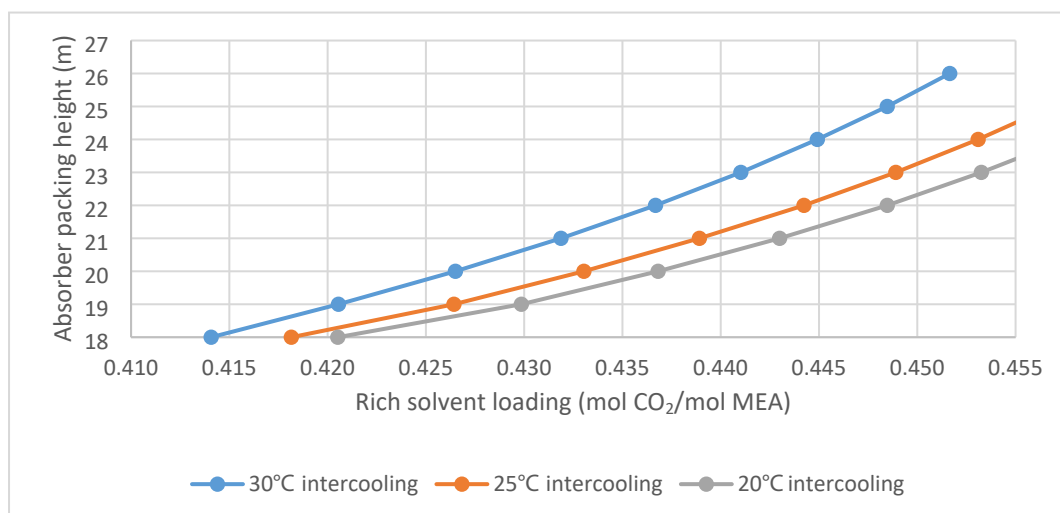

Fig. 9. Effect of absorber intercooling temperature on rich solvent loading and absorber packing height for achieving 99.72 % CO_2 capture rate with lean loading of 0.16 mol CO_2/mol MEA.

process, the temperature of the flue gas existing the air pollution control system is 136 °C, based on real operational data from a Recycling and Energy Recovery Centre (RERC) operated by FCC Environment in Edinburgh.

Up-stream of the DCC in the CO_2 capture plant, a gas–gas rotary heat exchanger is used to recover heat from the flue gas and increase the temperature of the CO_2-depleted gas from the absorber, ensuring adequate gas buoyancy and dispersion in the atmosphere.

The generic model of the 'power-only' configuration of a WtE plant was calibrated against the operating data of the Edinburgh RERC, with acceptable agreement. For detailed parameters used for the modelling, please refer to Appendix 2. The ultimate composition of the MSW was taken from the RERC data provided by FCC Environment, as shown in Appendix 3.

2.2.1.1. Capture plant modelling and ultra-high CO_2 capture rate. The

modelling methodology for the design and optimisation of the PCC process is illustrated in Fig. 5. The CO_2 capture plant is designed to process the total amount of flue gas exiting the WtE plant, i.e. a flue gas flow rate of 30.7 kg/s with a CO_2 concentration of 11.1 %vol downstream the DCC.

The overall CO_2 capture efficiency is defined as the amount of CO_2 captured for transport and storage/utilisation relative to the amount of CO_2 generated in the combustion of the waste. In this study, the operating and design parameters are evaluated for a range of CO_2 capture rates from 90 % to 99.72 %, taking as base case the design of a CO_2 capture process at 95 % CO_2 capture rate.

The upper limit of this range (99.72 % capture efficiency) is selected to represent an 'ultra-high' CO_2 capture rate that achieves zero-direct CO_2 emissions. In this scenario all the CO_2 produced in the combustion of the waste fuel is captured and the remaining CO_2 corresponds to the amount of CO_2 entering the process with the combustion air. For the
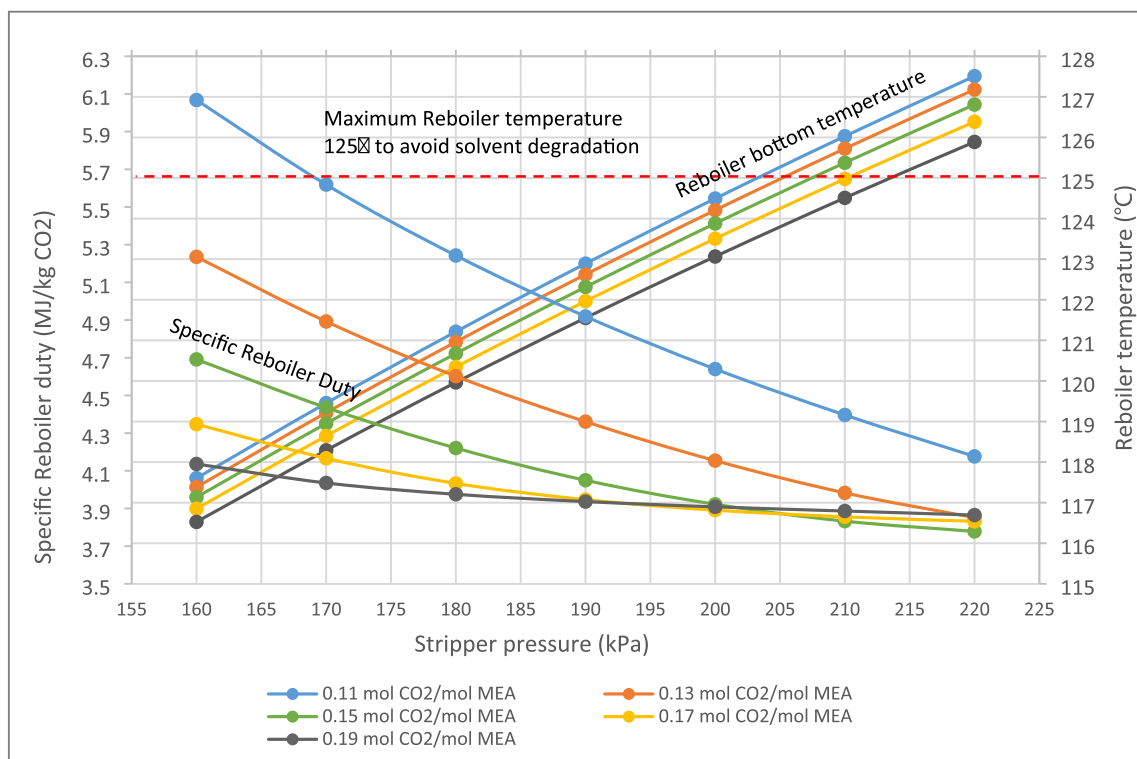
Fig. 10. Effect of stripper pressure on the specific reboiler duty for a range of lean solvent loadings. Under constant rich loading of 0.45 mol CO_2/mol MEA for 99.72 % CO_2 capture rate.

WtE plant treating 500 t/d of MSW, 5.168 kg/s of CO_2 exits the plant in the combustion gases, of which 99.72 % (5.15 kg/s) is captured in the PCC plant and the remaining 0.28 % CO_2 (0.0145 kg/s) corresponds to atmospheric CO_2 entering the plant with the combustion air.

In the 2nd step, the initial design parameters are considered in three sections: absorber, cross flow heat exchanger (XFHE) and regeneration.

In the absorption section, cooled flue gas downstream of the DCC is contacted with the solvent to remove CO_2 in a packed column. The absorber is a structured packing using Sulzer Standard Mellapak Plus 252Y with 35 % monoethanolamine (MEA) aqueous solution. Higher concentrations of MEA are reported to have lower SRD, especially at high CO_2 capture efficiency (e.g. a test campaign carried out at the Pilot Scale Advanced Capture Technology (PACT) facilities of the UK Carbon Capture and Storage Research Centre (UKCCSRC) [2]). The absorber column diameter is approximated using a method proposed by Chapel et al. [8], and a lean loading of 0.16 mol CO_2/mol MEA is initially assigned.

In the XFHE section, CO_2 'rich' solvent downstream of rich solvent pump (initially assigned 900kpa to avoid flashing) after the absorber is heated up against CO_2 'lean' solvent in the cross-flow heat exchanger before entering the stripper. The approach temperatures in the XFHE are specified to be 10 ℃.

Finally, in the regeneration section the CO_2 in the rich solvent is 'stripped off' by the condensing heat provided through the low-pressure saturated steam from the reboiler. The stripper operating pressure is designed to be 210 kPa with regeneration temperature around 125 °C to prevent thermal degradation, i.e. polymerisation. The conditions in the stripper are set to achieve the required CO_2 capture efficiency, under initial given lean solvent loadings. The temperature of the condensing steam in the reboiler exceeds the solvent temperature by the pinch temperature (10 °C) assumed in the reboiler design.

In the 3rd step, PCC plant simulation is performed with all the initial design parameters determined in the previous step. A range of absorber packing height is simulated for a constant diameter up to a value at which a further increase results in a marginal gain in the rich solvent

CO_2 loading and in a marginal reduction of the SRD (details provided in Section 3.1). The design absorber packing size (especially packing height), also needs to consider practical design limits that ensure efficient liquid dispersion and gas/liquid interactions within the packed bed to achieve the specified CO_2 capture efficiency.

Finally, in the optimisation step, the optimum lean solvent flow rate entering the absorber which minimises the SRD is evaluated for each CO_2 capture efficiency. Other parameters assigned during the initial input stage such as absorber intercooling, stripper pressure, etc., can also be further optimised to allow the minimized SRD for the specified CO_2 capture rates to be identified. The sizing and optimisation results of the PCC plant are presented in Section 3.1.

2.2.1.2. Options for advanced thermal integration of a WtE plant with PCC. A recent study identifying the Best Available Techniques for PPC prepared by [13] for the UK Environment Agency suggests that various heat recovery concepts may theoretically be viable (i.e. consistent with the 2nd Law of Thermodynamics); although capital cost and reliability, availability, maintainability, operability (RAMO) considerations and specific characteristics of the PCC system might constrain implementation. Following these recommendations, two thermal integration options for a WtE plant with PCC, considered as 'Basic thermal integration' and 'Advanced thermal integration', are considered in this article.

The basic thermal integration option includes minimum modifications to the existing heat exchanger network, which leads to no excess heat being recovered from the CO_2 capture process. The thermal energy required for solvent regeneration and the DH system is supplied by steam extracted from the steam cycle of the WtE plant.

The advanced thermal integration option introduces additional modifications in the heat exchanger network based on engineering judgment with the objective of maximizing the net power output for a power-only WtE plant and maximizing thermal output for a WtE-CHP plant equipped with PCC. Excess heat can be recovered from three locations in the PCC process: the compressor intercoolers, the stripper

Table 2
Design and performance parameters of the PCC plant at two CO$_2$ capture levels.

Parameter	Unit	Reference case	Net-zero emission case
CO$_2$ capture efficiency		**95 %**	**99.72 %**
Flue Gas			
Flue Gas Flow Rate	kg/s	30.7	30.7
Inlet Temperature	°C	40	40
CO$_2$ Concentration	Mole Fraction	11.1	11.1
Absorber			
Lean solvent flowrate	kg/s	63.8	69.9
Packing Height	m	18	24
Diameter	m	3.8	3.8
Packing Volume	m^3	215	286
Intercooler Return Temperature	°C	25	25
Absorber Flooding	%	68 %	76 %
Heat exchanger			
Rich Cold Solvent Inlet Temperature	°C	44	45
Rich Hot Solvent Outlet Temperature	°C	118	118
Lean Hot Solvent Inlet Temperature	°C	125	125
Lean Cold Solvent Outlet Temperature	°C	54	55
Rich Solvent pump			
Pressure increase *	kpa	1000	900
Stripper			
Packing Height	m	8	10
Diameter	m	2.5	2.5
Packing Volume	m^3	63	79
Stripper Flooding	%	62 %	68 %
Lean Solvent CO$_2$ Loading	mol CO$_2$/mol MEA	0.16	0.16
Rich Solvent CO$_2$ Loading	mol CO$_2$/mol MEA	0.47	0.46
Stripper Pressure	kPa	210	210
Reboiler temperature	°C	125	125.2
Specific Reboiler Duty (SRD)	MJ/kg CO$_2$	3.59	3.72

Note: * The output pressure of the rich solvent pump is adjusted to prevent from flashing in the lean-rich solvent heat exchanger.

overhead condenser and the DCC.

For power-only operation, the recovered heat is used to provide heat to feedwater in the FWH train, thus reducing the amount of steam extracted and increasing the power output from the steam cycle. For CHP operations, the recovered heat is used in the DH system. The DH water return splits into five streams: four of them are heated in heat exchangers from 60 °C to 80 °C using relatively high-temperature heat from the compressor intercoolers and the stripper overhead condensers. A fifth stream is heated to 77 °C by a heat pump and then by steam extraction to the final DH supply temperature of 80 °C. Steam condensation will occur for gas to liquid heat exchange, so the pinch temperature is set to be 15°C for heat recovery from the stripper overhead condenser. A schematic representation of the available heat sources in the PCC process and the thermally integrated configuration used in the advanced integration case is illustrated in Fig. 6.

The heat pump is used in the fifth stream to recover heat from DCC cooling water since the temperature level at the DCC is relatively low and, therefore, not high enough for direct use. Heat from DCC cooling water is recovered in the heat pump evaporator, increasing the DH water temperature from 60 °C to 77°C (through private communication with a heat pump vendor, this is the highest temperature for a commercially available single stage centrifugal compression heat pump and the COP of

the heat pump is approximated to be 5.5).

The heat pump can produce about 12MWth heat for DH, with a power consumption of about 2.2MWe. It should be noted that the COP of heat pump is closely related to the temperature lift (which is the temperature difference between condensing temperature and evaporating temperature) of the heat pump. For example, reducing the temperature lift can increase the COP, thus reducing the power consumption. The use of heat pumps in WtE plants with CCS has been proposed in several studies, such as the FEED study of the Oslo WtE-CHP plant [43], and a recent report by IEAGHG [21].

2.3. Key performance indicators for performance analysis

The following key performance indicators are defined in this article for the purpose of conducting a standardised performance evaluation and comparative assessment across the different WtE plant configurations investigated, without and with CCS.

2.3.1. Thermodynamic metrics for power-only configuration
Electricity output penalty (EOP).

EOP is evaluated as the total net loss in power output due to the CO$_2$ capture process divided by the mass flow of compressed CO$_2$ exiting the plant boundaries [28], as shown in Equation (1).

$$EOP = \frac{W_{e,ref} - W_{e,CCS}}{\dot{m}_{CO2,captured}} [MWh_e/t_{CO_2}] \tag{1}$$

Where: $W_{e,ref}$ Net power output without CCS [MW$_e$]. $W_{e,CCS}$ Net power output with CCS, considering reduction in steam turbine power output due to steam extraction for solvent regeneration, power consumption associated with the CO$_2$ capture process and any offsets due to beneficial heat recovery for condensate heating and other purposes [MW$_e$]. $\dot{m}_{CO2,captured}$ Mass flow of CO$_2$ captured exiting the plant boundaries [t/h].

Efficiency Penalty.

The efficiency penalty ($\Delta\eta$) is evaluated as the reduction in the net electrical efficiency of the WtE plant due to CO$_2$ capture and compression as shown in Equation (2). For a power only WtE plant with CO$_2$ capture, the net electrical efficiency is evaluated as the ratio of the net power output divided by the waste fuel thermal input on LHV basis.

$$\Delta\eta = \eta_{ref} - \eta_{CCS} \qquad = \frac{W_{e,ref}}{Q_{fuel\_input}} - \frac{W_{e,CCS}}{Q_{fuel\_input}} \tag{2}$$

Where: η_{ref}, η_{CCS} Electrical efficiency without and with CCS [-]. Q_{fuel_input} Fuel thermal input on LHV basis [MWh$_{th}$].

2.3.2. Thermodynamic metrics for CHP configuration
Energy utilisation factor (EUF) penalty.

EUF is evaluated as the ratio of the total energy output, including net useful electrical output and net useful thermal output, divided by the total fuel thermal input on LHV basis, as shown in Equation (3). This parameter facilitates the performance comparison of a CHP plant with and without CO$_2$ capture, but it does not differentiate between the exergy level of power and heat. The energy utilisation factor penalty (ΔEUF) is calculated as in Equation (4).

$$EUF = \frac{W_e + Q_{th,DH}}{Q_{fuel\_input}} = \frac{W_e + Q_{th,DH}}{Q_{fuel\_input}} \tag{3}$$

$$\Delta EUF = EUF_{ref} - EUF_{CCS} = \frac{W_{e,ref} + Q_{th,DH,ref}}{Q_{fuel\_input}} - \frac{W_{e,CCS} + Q_{th,DH,CCS}}{Q_{fuel\_input}} \tag{4}$$

where $Q_{th,DH}$ Net useful thermal output for district heating, subscripts '*ref*' and '*CCS*' represents $Q_{th,DH}$ under reference case and CCS case, respectively [MWh$_{th}$].

Effective electricity efficiency (EEE) penalty.

Table 3
Summary of key performance results of investigated steam cycle configurations for WtE with PCC considering different heat integrations and CO_2 capture rates.

	Unit	Without PCC		PCC - basic heat integration		PCC - Advanced heat integration	
Power-only configuration							
CO_2 capture rate				**95 %**	**99.72 %**	**95 %**	**99.72 %**
Power output	MW$_e$	15.3		10.0	9.6	10.6	10.1
Key performance indicators							
Electricity output penalty (EOP)	kWh$_e$/tCO$_2$			297	304	266	277
Efficiency penalty	–			9.4 %	10.2 %	8.5 %	9.3 %
Carbon intensity	gCO$_2$/kWh electrical	482		−1011	−1142	−959	−1086
	gCO$_2$/kg waste	353		−486	−528	−486	−528
CHP-Ex&C configuration							
CO_2 capture rate		*	†	**95 %***	**99.72 %†**	**95 %**	**99.72 %**
Power output	MW$_e$	12.5	12.8	7.2	7.1	5.0	4.9
Heat output	MW$_{th}$	14.1	12.5	14.1	12.5	32.2	31.4
Key performance indicators							
Energy utilisation factor (EUF) penalty	–	–	–	9.6 %	10.4 %	−19.0 %	19.6 %
Effective electricity efficiency (EEE) penalty	–	–	–	14.1 %	14.4 %	0.6 %	2.2 %
Carbon intensity	gCO$_2$/kWh electrical	589	573	−1415	−1553	−2035	−2246
	gCO$_2$/kWh thermal	523	587	−718	−877	−315	−350
	gCO$_2$/kg waste	353	353	−486	−528	−486	−528
CHP-BP configuration							
CO_2 capture rate				**95 %**	**99.72 %**	**95 %**	**99.72 %**
Power output	MW$_e$	8.12		6.25	6.17	4.1	4.0
Heat output	MW$_{th}$	37.3		19.9	18.5	38.0	37.3
Key performance indicators							
Energy utilisation factor (EUF) penalty	–	–	–	36.7 %	40.3 %	5.4 %	8.4 %
Effective electricity efficiency (EEE) penalty	–	–	–	68.6 %	70.0 %	34.0 %	45.1 %
Carbon intensity	gCO$_2$/kWh electrical	907	907	−1621	−1782	−2489	−2758
	gCO$_2$/kWh thermal	197	197	−509	−595	−267	−294
	gCO$_2$/kg waste	353	353	−486	−528	−486	−528

Note: For CHP-Ex&C configuration without PCC, the DH capacity for different CO_2 capture rate is different, since the DH capacity is calculated under the same minimum flow rate through the LP steam turbine of the power only WtE plant. The *,† indicates the reference CHP WtE without PCC considered for each capture rate, on the basis of maintaining the same thermal output when PCC is integrated.

Table 4
WtE with PCC EOP and Efficiency penalty for power only configuration.

		Unit	95 %	99.72 %
Electricity output penalty	Basic heat integration	MWh$_e$/tCO$_2$	297	304
	Advanced heat integration	MWh$_e$/tCO$_2$	266	277
Efficiency penalty	Basic heat integration	–	9.4 %	10.2 %
	Advanced heat integration	–	8.5 %	9.3 %

EEE allows a direct performance comparison between power only and CHP plants. It is defined here as the ratio between the net electrical output and the additional fuel that the CHP consumes above what would have been used by a conventional boiler to produce the thermal output of the CHP plant. EEE and EEE penalty (ΔEEE) is calculated as shown in Equation (5) and Equation (6).

$$EEE = \frac{W_e}{Q_{fuel\_input} - Q_{th,H}/\alpha} \quad (5)$$

$$\begin{aligned} \Delta EEE &= EEE_{ref} - EEE_{CCS} \\ &= \frac{W_{e,ref}}{Q_{fuel\_input} - Q_{th,\,DH\_ref}/\alpha} - \frac{W_{e,CCS}}{Q_{fuel\_input} - Q_{th,\,DH\_CCS}/\alpha} \end{aligned} \quad (6)$$

Whereα The efficiency of the conventional technology that would have been used to produce the useful thermal output if the CHP is not in place. This work assumes that the conventional technology is a grate boiler and assigns a constant value of 0.8.

2.3.3. Carbon intensity of a WtE plant equipped with PCC

In order to assess the potential for negative emissions of the CCS WtE sector, the carbon emission intensity is calculated on the basis of both electricity and thermal output. The biogenic carbon content in the referenced MSW incinerated is not available at the time of the writing and a 60 % biogenic to total carbon ratio is assumed in this study, based on a literature review in the public domain [14,24,36].

$$Carbon\,intensity_{fuel} = \frac{Fossil\,CO_2\,emitted - Biogenic\,CO_2\,captured}{Amount\,of\,MSW\,input\,(tons)} \quad (8)$$

$$Carbon\,intensity_{electrical} = \frac{Fossil\,CO_2\,emitted - Biogenic\,CO_2\,captured}{Net\,power\,output} \quad (9)$$

$$Carbon\,intensity_{thermal} = \frac{Fossil\,CO_2\,emitted - Biogenic\,CO_2\,captured}{Net\,thermal\,output} \quad (10)$$

3. Results and discussion

In this section, modelling results for three WtE plant configurations with PCC are presented, along with performance assessments based on metrics defined in Section 2.3.
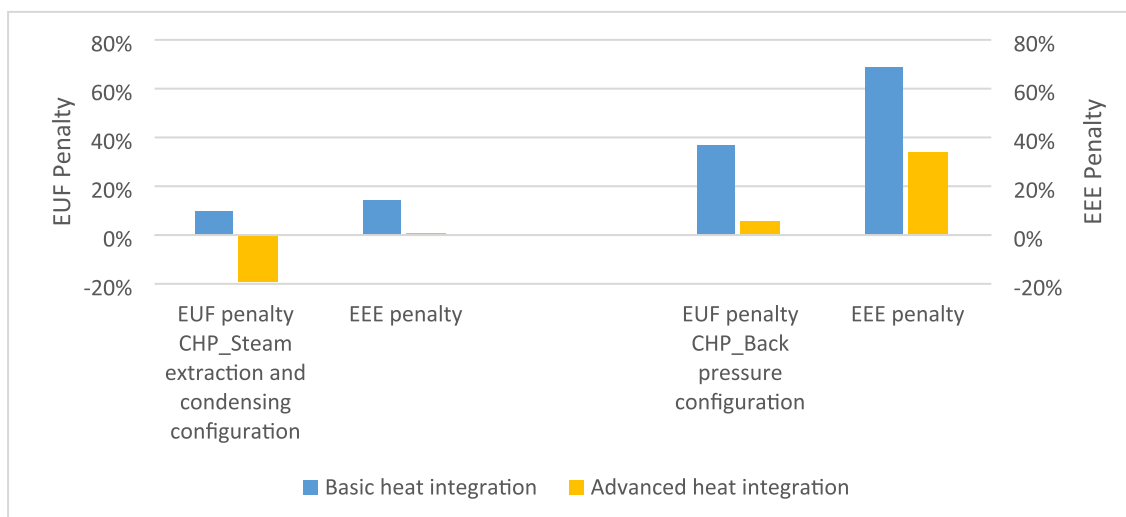
Fig. 11. Effect of heat recovery on the EUF penalty and the EEE penalty for a CHP WtE plant with PCC at 95% CO_2 capture rate.
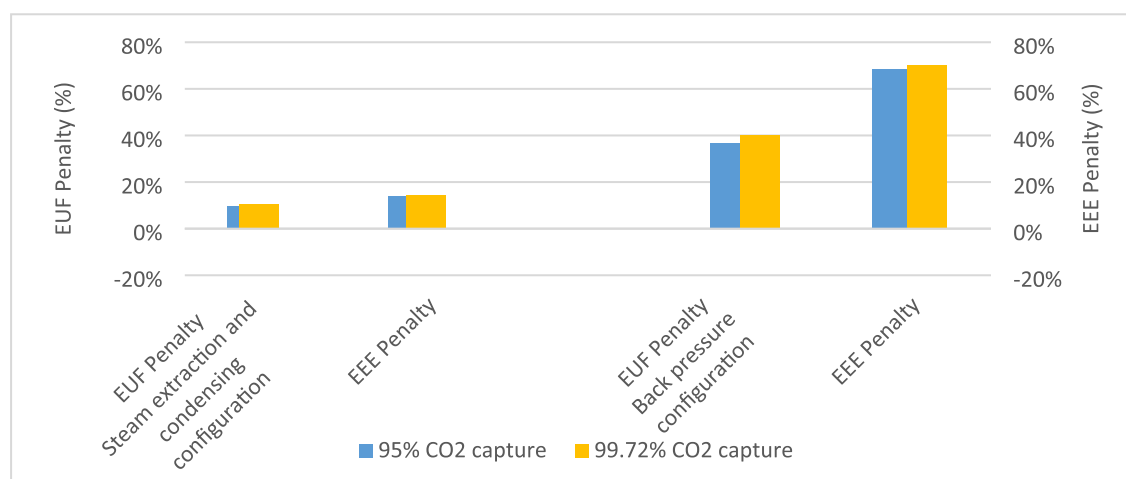

Fig. 12. Effect of Ultra-high CO_2 capture rate on the EUF penalty and the EEE penalty for a CHP WtE plant with PCC for two steam cycle configurations and basic heat integration.

Table 5
Carbon intensity on the basis of fuel input for different CO_2 capture efficiencies.

Carbon intensity	WtE without PCC	95 % CO_2 capture	99.72 % CO_2 capture
gCO_2/kg waste	353	−486	−528

3.1. Sizing and optimisation of the PCC system for a range of CO_2 capture efficiencies

The CO_2 capture plant is designed and optimised to process the total amount of flue gas exiting the WtE plant. The flue gas flow rate, temperature, pressure and composition at the inlet of the CO_2 capture systems are presented in Table 1. These data are used as input values for the Aspen Plus model of the PCC plant.

3.1.1. Absorber packing design and optimisation

Absorber design in PCC systems involves a trade-off between capital cost and operating cost. In general, a higher absorber packing bed or a higher SRD (specific reboiler duty) is required to achieve a higher CO_2 capture rate. Fig. 7 illustrates the effect of increasing the absorber packing height on SRD and on rich solvent loadings, for a range of CO_2 capture rates.

For a given CO_2 capture rate, a higher packing height results in a larger contact surface area and a longer residence time, which enhances the CO_2 absorption rate and thus the CO_2 loading of the solvent at the bottom of the absorber (rich solvent) increases. This also results in an increased solvent capacity for a given lean solvent CO_2 loading, and thus a reduced amount of solvent is required to achieve a given CO_2 absorption efficiency, which reduces the sensible heat required to heat the solvent to the reboiler temperature (once the solvent has been transferred to the stripper). This is reflected in a reduced SRD.

In this work, the absorber packing height is optimised for each one of the considered configurations separately to enable a fair comparison of technical performance. For each case, the absorber packing height is increased to a value at which a further increase in packing height results in a similar marginal (and small) gain in the rich solvent CO_2 loading and also a similar marginal (and small) reduction of the SRD. However, practical constraints need to be considered as well. Personal communications from SULZER suggested an upper limit of 8 m to 10 m for the height of each structured packing section (packing bed) in the absorber column to ensure adequate liquid distribution and structural integrity.

Using this approach, an absorber packing height of 24 m (3 packing beds of 8 m each) is selected for the net-zero direct emission case (i.e. 99.72 % capture rate); a further increase would lead to a marginal decrease in the SRD of 1.3 %. For the base case of 95 % capture rate an
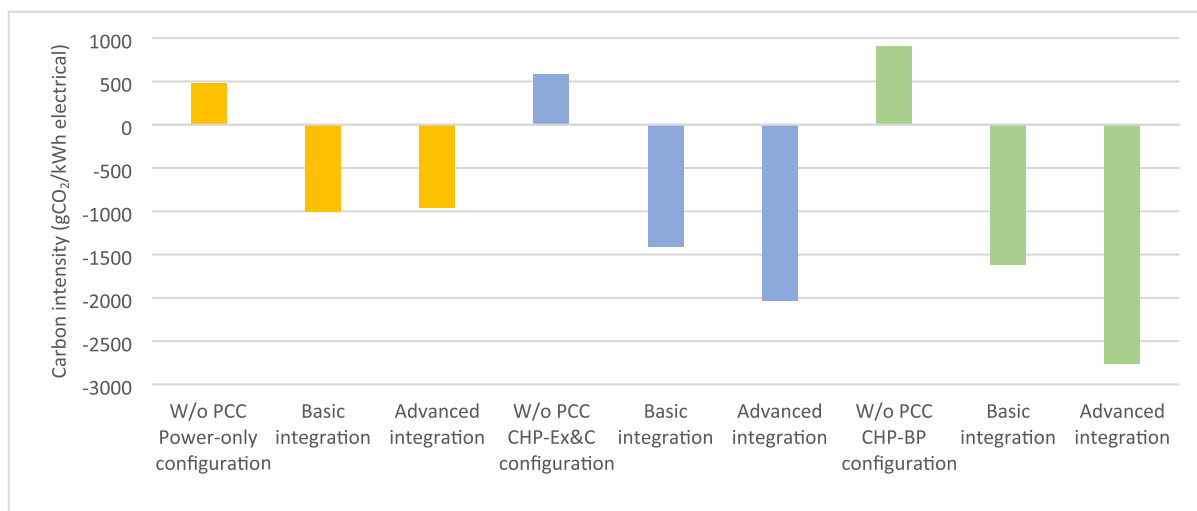
Fig. 13. Carbon intensity of a WtE plant without and with PCC at 95% CO$_2$ capture rate.
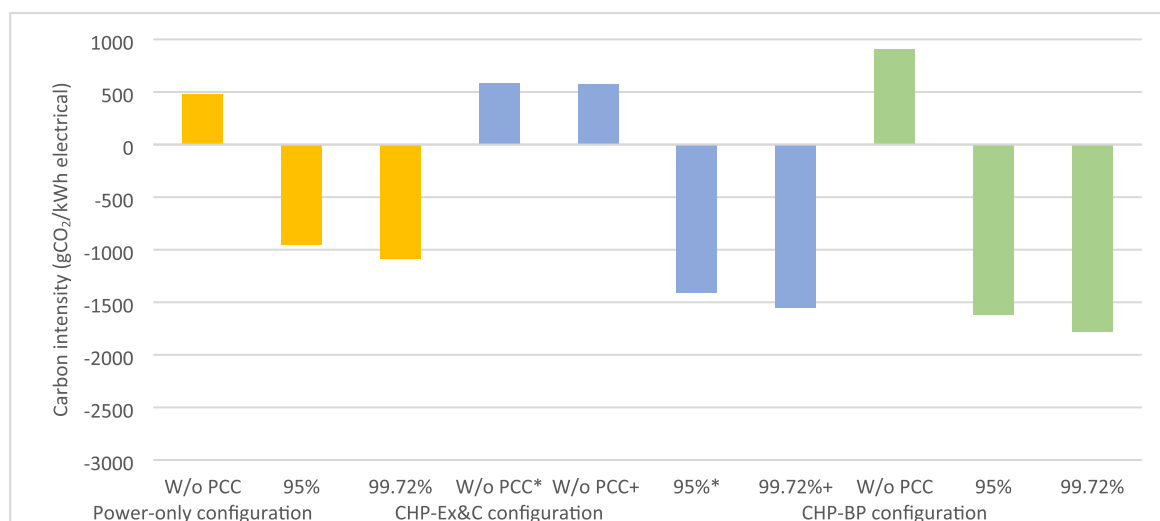

Fig. 14. Carbon intensity on the basis of net electricity output of a WtE plant without and with PCC at 95% and 99.7% CO$_2$ capture rates (Basic heat integration); in the figure, the signs *,† indicates the reference WtE without PCC on the basis of maintaining the same thermal output with PCC is added for each capture rate.

absorber packing height of 18 m (two packing sections of 9 m each) is selected, leading to a similar marginal decrease in the SRD of 1.4 %.

3.1.2. Effect of lean solvent loadings

The effect of lean solvent CO$_2$ loading on the SRD and L/G ratio is illustrated in Fig. 8 for a range of CO$_2$ capture efficiencies 95 %/99 %/99.72 %, with absorber packing height initially assigned of 17 m/20 m/22 m respectively. At a lower lean solvent CO$_2$ loading, a smaller amount of solvent is required to achieve a certain CO$_2$ capture rate, yet the contribution of the heat of desorption to the SRD is more relevant. At a higher lean solvent CO$_2$ loading, more solvent is required to achieve a certain CO$_2$ capture rate, and thus the effect of sensible heat required to heat the solvent to the stripper temperature on the reboiler duty becomes more significant. There is therefore an optimal value of the lean solvent CO$_2$ loading that results in a minimum SRD.

3.1.3. Effect of absorber intercooling

Absorber intercooling enables a shift in the thermodynamic vapour-liquid equilibrium, ensures high driving forces for CO$_2$ mass transfer through the column and consequently increases the rich solvent loading at the bottom of the absorber [33]. The intercooling temperature has

been typically set at 40℃ for 90 % CO$_2$ capture rate [37]. Intercooling temperatures between 30℃ and 40℃ have been used for 99 % capture level in recent studies [12]. [31] report that the impact of intercooling on the rich loading is greater at higher lean loadings for 99 % capture level.

The design of the capture plant conducted in this study shows that absorber intercooling is necessary for achieving ultra-high CO$_2$ capture rates above 99 %. If intercooling is not implemented, the large amount of heat released leads to a significant high temperature bulge at the top of the absorber column, reducing the driving force for CO$_2$ transfer. For a given rich solvent loading, applying intercooling also decreases the required absorber packing height. As shown in Fig. 9, lower intercooling temperature allows the absorber column to have a closer approach to equilibrium, leading to lower SRD. In this study, the intercooler is located after the first top packing section for 95 % CO$_2$ capture (two packing sections of 9 m each) and 99.72 % CO$_2$ capture (three packing sections of 8 m each). The solvent exits the absorber column at the end of the first packing section, passes through an external heat exchanger where it is cooled down to 25℃ and returns to the column at the top of the second packing section.
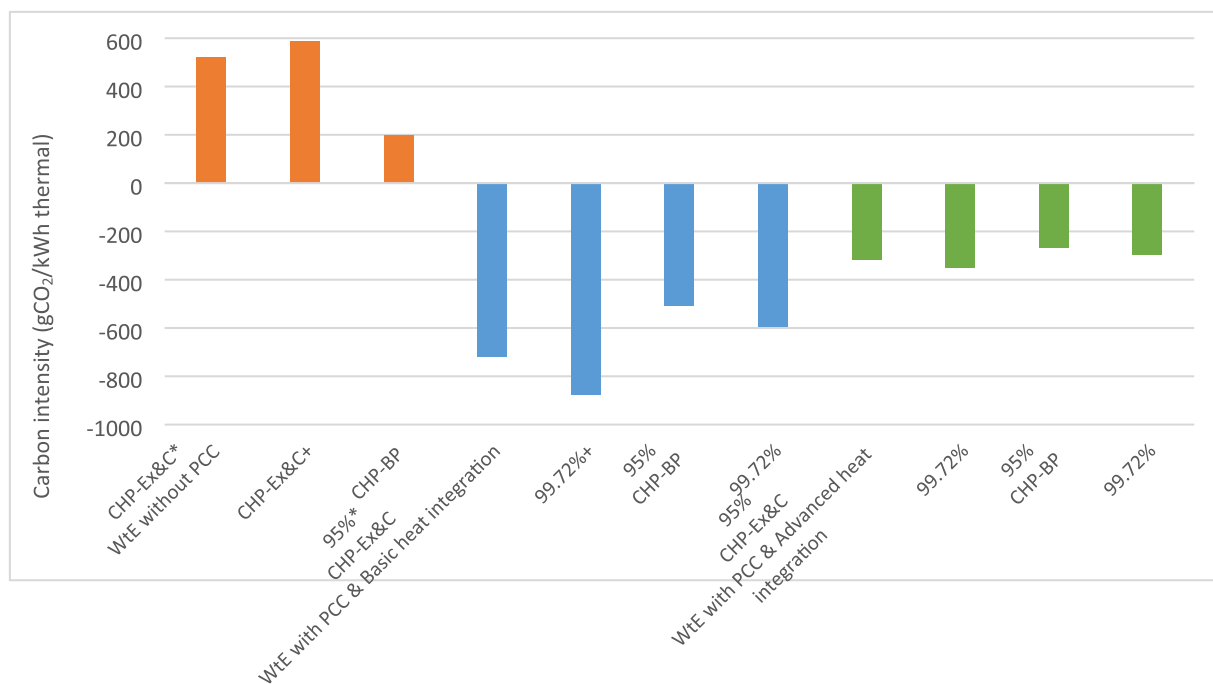
Fig. 15. Carbon intensity on the basis of thermal output for a CHP WtE plant without and with PCC for a basic and an advanced thermal integration; in the figure, the signs *,† indicates the reference WtE without PCC on the basis of maintaining the same thermal output with PCC is added for each capture rate.

3.1.4. Effect of stripper pressure

The effect of the stripper pressure on the SRD for a range of lean solvent loadings is also investigated as part of the optimisation of the PCC plant design. Fig. 10 shows that at higher stripper pressures, the effect of the lean solvent loading on the SRD is less significant and the SRD required to achieve a given lean solvent loading is smaller. A higher stripper pressure requires, however, a higher reboiler temperature to generate the steam to strip CO_2 from the loaded solvent. Therefore, there is a maximum stripper pressure above which the required reboiler temperature would be higher than the limiting temperature that accelerates thermal degradation of the solvent.

According to the VLE curve, increasing temperature will increase CO_2 partial pressure in the stripper, so the CO_2 fraction at the top of the stripper increases, while the vapour fraction at the top of the stripper decreases. Additionally, the absolute values of both CO_2 partial pressure and vapour partial pressure increase with increase of stripper pressure. A lower vapour fraction at the top leads to a lower heat lost due to vaporization, so the SRD is smaller at higher stripper pressures.

For a constant stripper pressure, on one hand, a lower lean solvent loading leads to a higher solvent capacity and a smaller amount of solvent required to achieve a certain CO_2 capture rate, e.g., 99.72 %, and thus the contribution of the sensible heat required to increase solvent temperature to the stripper temperature decreases. On the other hand, a higher heat of desorption is required to achieve a lower lean solvent loading. The overall effect is an increase in the SRD to achieve lower lean loadings at a constant stripper pressure which becomes more significant at very low lean solvent loadings. This implies that when designing the PCC plant with lower lean loadings, in order to minimize SRD, increasing stripper pressure (to a level that does not exceed solvent degradation temperature) should be considered.

3.1.5. Summary of PCC plant modelling results

Based on the design and optimisation procedure reported in this section, the key parameters of the CO_2 capture plant for the 95 % and 99.72 % CO_2 capture efficiency are presented in Table 2. The capture plant data obtained from the PCC system modelled in Aspen Plus are used as input parameters to the WtE plant model in gProcess to assess the

effect of increasing the CO_2 capture efficiency on the performance of the WtE plant.

3.2. Summary of the technical performance and KPI results of WtE with PCC integration

A summary of the results from the performance assessment of the investigated scenarios of a WtE with PCC described in Section 2.2 are presented in Table 3. It shows the effects of different heat integration options and CO_2 capture rates on the net power and thermal output from the WtE plant and the KPI values identified in Section 2.3. Under these configurations, the key plant specific parameters such as the steam outlet parameters from boiler, waste throughput into the system, low pressure turbine swallowing capacity, etc., remains the same. The KPI results will be discussed separately in Section 3.3.

The reduction in the net power output when PCC is implemented accounts for (1) the power reduction due to steam extraction from steam cycle for solvent regeneration; (2) the power consumption in the CO_2 compression train, and (3) power reduction due to ancillary power consumption such as booster fan, solvent pumps, etc. As can be seen from the Table 3, under CHP-Ex&C configuration, the WtE plant can be operated to maintain the same DH capacity when CO_2 capture is implemented, yet the DH capacity will slightly decrease at higher CO_2 capture rates. On the other hand, under CHP-BP configuration, the WtE plant is operating at the maximum heat to power ratio, adding PCC would considerably reduce the net useful thermal output from 37.3 MW_{th} in the reference configuration down to 18.5 MW_{th} for 99.7 % CO_2 capture ratio.

The amount of heat that could potentially be recovered from the CO_2 compressor intercoolers, stripper overhead condenser and DCC (recovered by the heat pump, as discussed in Section 2.2.3) is 1.6 MW, 5.3 MW and 9.8 MW respectively. For CHP plants with advanced heat integration, the DH capacity is increased by recovering much of this heat. For example, for the CHP-Ex&C configuration, an advanced thermally integrated WtE plant could overcome the reduction in net useful thermal output when CO_2 capture is used with only basic heat integration. For CHP-BP configuration, the WtE plant is operating at the maximum heat

to power ratio, adding a PCC system would not compromise the net useful thermal output, i.e. 37.3 MW$_{th}$ at 99.7 % CO_2 capture level compared to the same value for the reference case without PCC.

3.3. Assessment of the thermodynamic metrics of WtE facilities with PCC

3.3.1. Power-only WtE plant

The assessment of the performance of the power-only WtE plant with PCC is presented in terms of electricity output penalty (EOP) and efficiency penalty in Table 4. It can be seen that in general, heat recovery can effectively reduce the energy penalty associated with PCC integration. With basic heat integration, the EOP is ca. 297kWh/kgCO$_2$ and 304kWh/kgCO$_2$ at 95 % and 99.72 % CO_2 capture rate respectively, which results in corresponding efficiency penalties of 9.4 % and 10.2 %. For advanced heat integration, the EOP is reduced to 266 kWh/kgCO$_2$ and 277 kWh/kgCO$_2$, a 31kWh/kgCO$_2$ and 27 kWh/kgCO$_2$ reduction respectively.

Heat recovery into the FWH train is constrained at 99.72 % CO_2 capture level. In this case, more steam is extracted from steam cycle, leading to a higher mass flowrate reduction of boiler condensate in the FWH, which reduces the capacity of boiler condensate to absorb the heat available in the stripper overhead condenser.

Comparing with the reference case (95 % CO_2 capture rate), the net-zero emission case (99.72 % CO_2 capture rate) shows slightly higher EOP and efficiency penalty, but the difference is relatively small when compared to the effect of heat recovery on system performance.

3.3.2. CHP WtE plants

The assessment of the performance of a CHP WtE plant with PCC is presented here in terms of energy utilisation factor (EUF) penalty and effective electricity efficiency (EEE) penalty with results illustrated in Fig. 11 and Fig. 12.

The CHP-BP configuration has the highest EUF and EEE before and after CO_2 capture. This is because there are no condensing heat losses in this configuration. The low pressure turbine and condenser is bypassed in order to provide as much heat as possible. When CO_2 capture is integrated with basic heat integration, both EUF and EEE are reduced. As shown in Fig. 11, for basic heat integration, the EUF penalty is about 9.6 % and 37 % for CHP-Ex&C and CHP-BP configurations respectively. The EEE penalty for the two CHP configurations are about 14 % and 69 % respectively.

Advanced heat integration greatly improves the situation. The EUF penalty is reported as a negative value for the CHP-Ex&C configuration, which means that EUF is improved in comparison to a case without CO_2 capture. This is due to about 17MWth of heat being recovered from the PCC process (EEE is not increased so significantly, since besides EOP of CO_2 capture, additional power consumption is required for the heat pump to recover heat from DCC). For CHP-BP configuration, the EUF penalty and EEE penalty are both decreased with advanced heat recovery, but still positive value which means the EUF and EEE is still lower than for an equivalent plant operating without CO_2 capture.

Fig. 12 shows the effect of Ultra-high CO_2 capture rate on the CHP performance under basic heat integration. It can be seen that for the two CHP configurations, the effect of higher CO_2 capture rate is marginal. A similar trend is observed under advanced heat integration. In general, comparing the effect of heat recovery and ultra-high CO_2 capture rate on CHP performances, the effect of heat recovery strategy is much more significant than choice of CO_2 capture rate.

Assessment of the carbon intensity of WtE facilities with PCC.

As outlined in Section 2.3.3, in this work the carbon intensity of a WtE plant with PCC is evaluated on the basis of net direct CO_2 emissions per unit of fuel input, per unit of electricity output and per unit of thermal output.

3.3.3. Carbon intensity on the basis of fuel input

The amount of MSW treated is assumed to be constant for all the investigated configurations, so the carbon intensity on the basis of fuel input only varies with the CO_2 capture efficiency. For a MSW composition with a total carbon content of 250 kg per tonne of MSW, on wet basis, a biogenic carbon ratio of 60 %, an ash content of 222 kg/t MSW incinerated and a loss of ignition (LOI) of 10 %, total direct CO_2 emissions from fuel combustion are 891 kg/t MSW, of which 535 g CO_2/kg MSW are of biogenic origin, and considered to be carbon neutral, and 353 g CO_2/kg MSW are of fossil origin. When the WtE is equipped with PCC, the amount of biogenic CO_2 captured and permanently stored leads to 'negative' carbon emissions as presented in Table 5.

3.3.4. Carbon intensity on the basis of electricity output

Fig. 13 and Fig. 14 presents the carbon intensity on the basis of the net electricity output for the three investigated configurations of the WtE plant without and with PCC. Fig. 13 focuses on the effect of heat recovery and Fig. 14 focuses on the effect of the CO_2 capture rate on the carbon intensity.

The carbon intensity of the power only WtE facility without PCC modelled in this work is approximately 482 gCO$_2$/kWh$_e$, similar to the global average of 475 gCO$_2$/kWh$_e$ reported by IEA [19]. This value is higher for CHP WtE facilities operating at higher heat to power ratios, since the net power output is smaller. For a CHP WtE with a back pressure steam turbine (i.e. highest possible heat to power ratio), the carbon intensity is approximately 907 gCO$_2$/kWh$_e$. Implementing CO_2 capture and permanent storage to a WtE plant considerably reduces the carbon intensity leading to net negative CO_2 emissions. For example, the power-only WtE plant with CO_2 capture in Fig. 13 removes between 960 and 1010 gCO$_2$ per kWh of exported electricity, with the variation in CO_2 removal caused by the heat integration approach chosen.

CHP WtE plants with PCC present a lower carbon intensity than power-only WtE plants for the same CO_2 capture rate since the power output is lower. Advanced heat recovery introduces a higher power output penalty leading to a lower carbon intensity, as shown in Fig. 13. Increasing the capture rate leads to a real reduction in the carbon intensity, as shown in Fig. 14, since the additional biogenic CO_2 captured balances the relatively small increase in the power output penalty at higher CO_2 capture levels.

3.3.5. Carbon intensity on the basis of thermal energy output

Adding PCC to a CHP WtE plant reduces the net useful thermal energy output for district heating. Fig. 15 presents the carbon intensity on the basis of the net thermal energy output for the two configurations of a CHP WtE plant at different CO_2 capture rates. The absolute values of negative carbon intensity are higher for a CHP WtE plant operated at smaller heat to power ratios. Higher CO_2 capture rate leads to higher negative CO_2 emissions for the same amount of total fuel consumption in the WtE plant. Heat recovery reduces the absolute values of negative carbon intensity, since for the same amount of CO_2 captured the thermal energy output significantly increases due to the heat recovered from the process.

4. Conclusions

This paper presents a series of modelling activities focussed on WtE plants integrated with PCC systems using 35 %wt monoethanolamine (MEA) aqueous solution. The overall process is modelled in gProcess software with the CO_2 capture plant modelled in detail in ASPEN Plus, starting from a CCSI open-source steady-state model developed by the US DOE. A set of KPIs are identified and reported for performance assessment for each scenario considered in the analysis. Modelling scenarios are chosen to explore the potential of ultra-high CO_2 capture and advanced heat recovery for CHP-type WtE plants using PCC. Results show that intercooling is necessary at the investigated lean loading to achieve the targeted ultra-high capture rate (99.72 % to achieve zero direct CO_2 emissions). When compared with the 95 % capture base case, ultra-high capture levels have marginal impacts across all the relevant

metrics used in this paper indicating that ultra-high capture levels can be achieved in the WtE sector.

This study also shows that WtE CHP plant performance with PCC is significantly improved by using advanced heat recovery from the PCC process. The advanced heat recovery configuration developed for this study is able to offset the energy penalty due to heat and power requirements from the capture plant when advanced heat integration at 99.72 % capture level is compared to basic heat integration at 95 % capture level. In the CHP-Ex&C configuration with advanced heat recovery, the EUF is higher than the same WtE plant without CO_2 capture due to the substantial use of heat that would otherwise be wasted. Implementing PCC systems at WtE facilities considerably reduces the carbon intensity of these facilities. This study highlights the importance of careful considerations of carbon intensity metrics on different bases when the carbon intensity of WtE plants equipped with PCC are compared with other waste management options or with alternative sources of electricity and/or heat. The absolute amount of negative emissions of integrated WtE PCC systems only change when CO_2 capture rate is changed. Some metrics reporting carbon intensity do, however, change significantly between cases due to changes in net power and/or heat output. For example, with advanced heat recovery, the system is reported to have the lowest carbon intensity on electricity basis, but the highest carbon intensity on thermal basis. It is, therefore, important that a comprehensive set of performance metrics is used when WtE PCC systems are compared with other negative emissions technologies.

CRediT authorship contribution statement

Dan Su: Conceptualization, Data curation, Methodology, Software, Writing – original draft. **Laura Herraiz:** Software, Validation, Writing – review & editing. **Mathieu Lucquiaud:** Conceptualization, Investigation, Supervision, Visualization. **Camilla Thomson:** Investigation, Writing – review & editing. **Hannah Chalmers:** Investigation, Methodology, Supervision, Writing – review & editing.

Declaration of Competing Interest

The authors declare that they have no known competing financial interests or personal relationships that could have appeared to influence the work reported in this paper.

Data availability

Data will be made available on request.

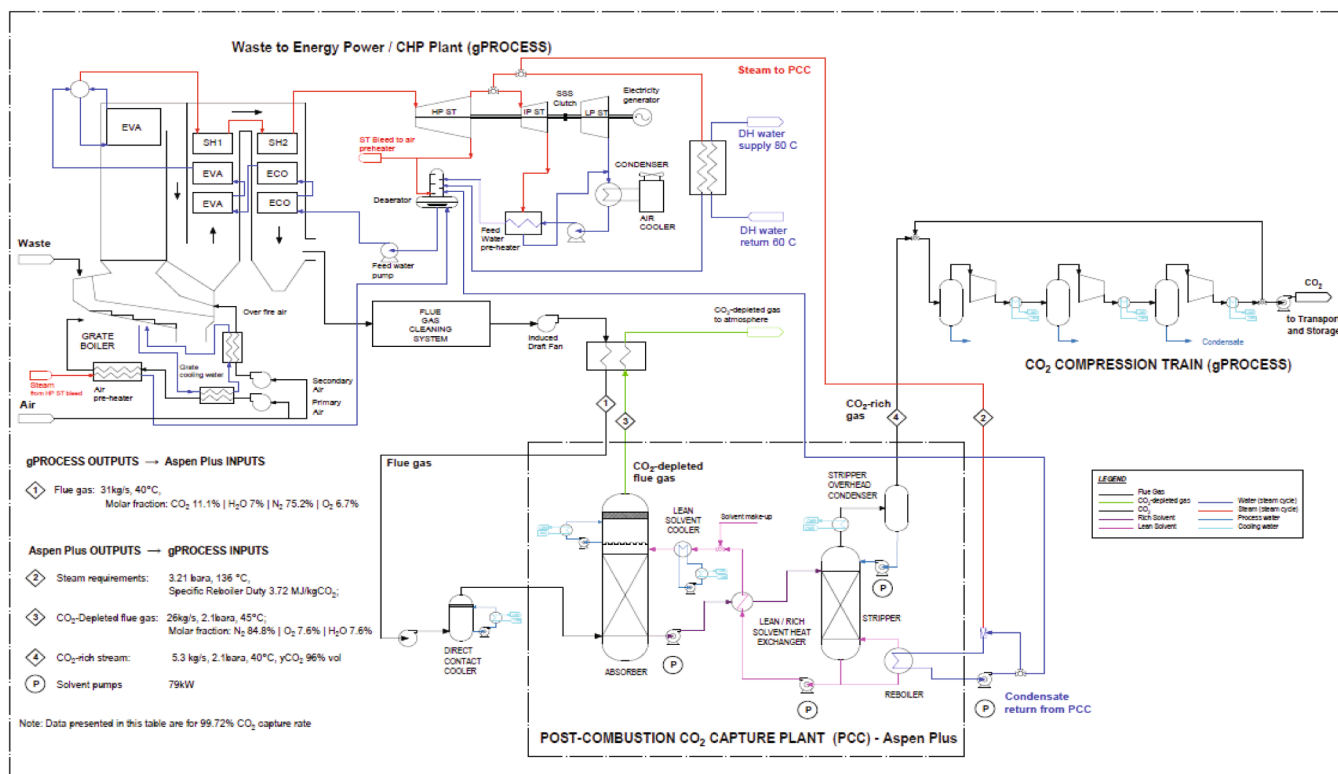**Appendix 1. . Process flow of WtE plant integration with Post-combustion CO_2 capture plant**

.

Appendix 2. . Design and operating parameters of the reference WtE plant

	Unit	gProms modelling
LHV	kJ/kg	9300
Waste throughput	t/h	19.4
Primary air into boiler	℃	135
Primary air mass-flow	kg/s	19.7
Primary air preheating (external)	MW	1.7
Secondary air into boiler	℃	50
secondary air mass-flow	kg/s	8.5
Secondary air preheating (external)	MW	0
Total air preheating from steam cycle	MW	1.7
Boiler Live steam Temperature	℃	400
Boiler Live steam pressure	bar	40
Boiler Live steam mass flowrate	kg/s	18.2
FW return Temperature	℃	137
FW return Pressure	bar	80
FW return mass flowrate	kg/s	18.2
Flue gas Temperature	℃	136
Flue gas pressure	bar	1
O_2 concentration in the flue gas		6.12 %
Boiler efficiency		88.0 %
Total thermal input	MW	55.6
Gross power output (w/o Carbon capture)	MW	15.7

Appendix 3. . MSW ultimate composition (as received) based on sampling in March 2019

Analyte	Units	Results
Moisture	% Wt	35.04
Ash	% Wt	22.19
Gross CV	MJ/kg	10.87
Net CV	MJ/kg	9.26
Oxygen	% Wt	13.53
Carbon	% Wt	25.02
Hydrogen	% Wt	3.19
Nitrogen	% Wt	0.66
Sulphur	% Wt	0.09
Chlorine	% Wt	0.28

References

[1] AECOM. (2021). Next Generation Carbon Capture Technology, Technoeconomic Analysis, Work Package 6, Department for Business, Energy and Industrial Strategy.

[2] Akram M, Milkowski K, Gibbins J, Pourkashanian M. Comparative energy and environmental performance of 40 % and 30 % monoethanolamine at PACT pilot plant. Int J Greenhouse Gas Control 2020;95. https://doi.org/10.1016/j.ijggc.2019.102946.

[3] Ayyad A, Abbas A, Elminshawy N. A simulation study of the effect of post-combustion amine-based carbon-capturing integrated with solar thermal collectors for combined cycle gas power plant. Discover Sustainability 2021;2(1). https://doi.org/10.1007/s43621-021-00018-x.

[4] Barba D, Brandani F, Capocelli M, Luberti M, Zizza A. Process analysis of an industrial waste-to-energy plant: theory and experiments. Process Saf Environ Prot 2015;96:61–73. https://doi.org/10.1016/j.psep.2015.04.007.

[5] Berry, J., & Attix, R. (2017). Economics of Overrunning Clutches to Automatically Connect and Disconnect Steam Turbines in CHP Systems, IDEA's 30th Annual Campus Energy Conference. Retrieved from https://www.districtenergy.org/HigherLogic/System/DownloadDocumentFile.ashx?DocumentFileKey=1dc317f5-88ac-b046-4ea7-2e59ba99b693.

[6] Branchini, L. (2015). Waste to energy advanced cycles and new design concepts for efficient power plants.

[7] Connolly D, Lund H, Mathiesen BV, Werner S, Möller B, Persson U, et al. Heat Roadmap Europe: combining district heating with heat savings to decarbonise the EU energy system. Energy Policy 2014;65:475–89. https://doi.org/10.1016/j.enpol.2013.10.035.

[8] Dan G. Chapel, C. L. M., John Ernest. Recovery of CO_2 from flue gases, Commercial trends, Canadian Society of Chemical Engineers Annual Meeting. 1999.

[9] Danaci D, Bui M, Petit C, Mac Dowell N. En route to zero emissions for power and industry with amine-based post-combustion capture. Environ Sci Technol 2021;55 (15):10619–32. https://doi.org/10.1021/acs.est.0c07261.

[10] De Greef J, Verbinnen B, Van Caneghem J. Waste-to-energy: coupling waste treatment to highly efficient CHP. Int J Chem Reactor Eng 2018;16(10). https://doi.org/10.1515/ijcre-2017-0248.

[11] Eboh FC, Ahlström P, Richards T. Evaluating improvements in a waste-to-energy combined heat and power plant. Case Stud Therm Eng 2019;14. https://doi.org/10.1016/j.csite.2019.100476.

[12] Gao T, Selinger JL, Rochelle GT. Demonstration of 99% CO_2 removal from coal flue gas by amine scrubbing. Int J Greenhouse Gas Control 2019;83:236–44. https://doi.org/10.1016/j.ijggc.2019.02.013.

[13] Gibbins J, Lucquiaud M. BAT Review for New-Build and Retrofit Post-Combustion Carbon Dioxide Capture Using Amine-Based Technologies for Power and CHP Plants Fuelled by Gas and Biomass as an Emerging Technology under the IED for the UK, UKCCSRC Report, Ver.1.0, July 2021. (https://ukccsrc.ac.uk/best-available-technology-bat-information-for-ccs/). 2021.

[14] GIOUSE F, RAVACHE E, MOUTTE L, LOUIN L, PARMENTIER E, WATIEZ K. DÉTERMINATION DES CONTENUS BIOGÈNE ET FOSSILE DES ORDURES MÉNAGÈRES RÉSIDUELLES ET D'UN CSR, A PARTIR D'UNE ANALYSE 14C DU CO2 DES GAZ DE POST-COMBUSTION. Program. UIOM 14C – Camp. Mes. sur UIOM chaufferie CSR. 2020.

[15] Gustafsson K, Sadegh-Vaziri R, Grönkvist S, Levihn F, Sundberg C. BECCS with combined heat and power: assessing the energy penalty. Int J Greenhouse Gas Control 2021;108. https://doi.org/10.1016/j.ijggc.2020.103248.

[16] Haaf M, Anantharaman R, Roussanaly S, Ströhle J, Epple B. CO_2 capture from waste-to-energy plants: techno-economic assessment of novel integration concepts of calcium looping technology. Resour Conserv Recycl 2020;162. https://doi.org/10.1016/j.resconrec.2020.104973.

[17] Hasan S, Abbas AJ, Nasr GG. Improving the carbon capture efficiency for gas power plants through amine-based absorbents. Sustainability 2020;13(1). https://doi.org/10.3390/su13010072.

[18] Hirata T, Tsujiuchi T, Kamijo T, Kishimoto S, Inui M, Kawasaki S, et al. Near-zero emission coal-fired power plant using advanced KM CDR process™. Int J Greenhouse Gas Control 2020;92. https://doi.org/10.1016/j.ijggc.2019.102847.

[19] IEA. Global Energy and CO_2 Status Report 2018. 2019.

[20] IEAGHG. ''Towards Zero Emissions from CCS Power Stations Using High Capture Rate or Biomass'', 2019/2, March. 2019.

[21] IEAGHG. CCS on Waste to Energy. 2020.

[22] Josh Morgan BO, Debangsu Bhattacharyya, Anuja Deshpande. CCSI Steady State MEA Model (MEA ssm) User Manual, Version 3.2.0, February 2021. Retrieved from https://github.com/CCSI-Toolset/MEA_ssm. 2021.

[23] Kärki J, Tsupari E, Arasto A. CCS feasibility improvement in industrial and municipal applications by heat utilisation. Energy Procedia 2013;37:2611–21. https://doi.org/10.1016/j.egypro.2013.06.145.

[24] Kaza S, Lisa Yao, Perinaz Bhada-Tata, Frank, Woerden V. What a Waste 2.0: A Global Snapshot of Solid Waste Management to 2050. *Urban Development Series. Washington, DC: World Bank.* doi:10.1596/978-1-4648 -1329-0. 2018.

[25] Kiani A, Jiang K, Feron P. Techno-economic assessment for CO_2 capture from air using a conventional liquid-based absorption process. Front Energy Res 2020;8. https://doi.org/10.3389/fenrg.2020.00092.

[26] Koukouzas N, Christopoulou M, Giannakopoulou PP, Rogkala A, Gianni E, Karkalis C, et al. Current CO_2 capture and storage trends in europe in a view of social knowledge and acceptance. A short review. *Energies* 2022;15(15). https://doi.org/10.3390/en15155716.

[27] Lombardi L, Carnevale EA. Evaluation of the environmental sustainability of different waste-to-energy plant configurations. Waste Manag 2018;73:232–46. https://doi.org/10.1016/j.wasman.2017.07.006.

[28] Lucquiaud M, Gibbins J. On the integration of CO_2 capture with coal-fired power plants: a methodology to assess and optimise solvent-based post-combustion capture systems. Chem Eng Res Des 2011;89(9):1553–71. https://doi.org/10.1016/j.cherd.2011.03.003.

[29] Magnanelli E, Mosby J, Becidan M. Scenarios for carbon capture integration in a waste-to-energy plant. Energy 2021;227. https://doi.org/10.1016/j.energy.2021.120407.

[30] Matak N, Tomić T, Schneider DR, Krajačić G. Integration of WtE and district cooling in existing Gas-CHP based district heating system – Central European city perspective. Smart Energy 2021;4. https://doi.org/10.1016/j.segy.2021.100043.

[31] Michailos S, Gibbins J. A modelling study of post-combustion capture plant process conditions to facilitate 95–99% CO_2 capture levels from gas turbine flue gases. Front Energy Res 2022;10. https://doi.org/10.3389/fenrg.2022.866838.

[32] Morgan JC, Soares Chinen A, Omell B, Bhattacharyya D, Tong C, Miller DC, et al. Development of a rigorous modeling framework for solvent-based CO_2 capture. Part 2: steady-state validation and uncertainty quantification with pilot plant data. Ind Eng Chem Res 2018;57(31):10464–81. https://doi.org/10.1021/acs.iecr.8b01472.

[33] Moullec YL, Neveux T. Process modifications for CO2 capture. In *Absorption-Based Post-combustion Capture of Carbon Dioxide* (pp. 305-340). 2016.

[34] NEWEST-CCUS. Oslo's Klemetsrud project secures financing in significant boost for waste-to-energy and CCS. Retrieved from https://www.newestccus.eu/news/oslo%E2%80%99s-klemetsrud-project-secures-financing-significant-boost-waste-energy-and-ccs. 2022.

[35] Reimann DO. CEWEP Energy Report III, Results of Specific Data for Energy, R1 Plant Efficiency Factor and NCV of 314 European Waste-to-Energy (WtE) Plants. 2013.

[36] REMONDIS. Production and use of Solid Recovered Fuels - developments and prospects. Retrieved from, https://bgs-ev.de/wp-content/uploads/2015/02/AFR_Remondis-Glorius_final_280814.pdf; 2014.

[37] Rezazadeh F, Gale WF, Rochelle GT, Sachde D. Effectiveness of absorber intercooling for CO_2 absorption from natural gas fired flue gases using monoethanolamine solvent. Int J Greenhouse Gas Control 2017;58:246–55. https://doi.org/10.1016/j.ijggc.2017.01.016.

[38] Rosa L, Sanchez DL, Mazzotti M. Assessment of carbon dioxide removal potential via BECCS in a carbon-neutral Europe. Energy Environ Sci 2021;14(5):3086–97. https://doi.org/10.1039/d1ee00642h.

[39] Roussanaly S, Ouassou JA, Anantharaman R, Haaf M. Impact of uncertainties on the design and cost of CCS from a waste-to-energy plant. Front Energy Res 2020;8. https://doi.org/10.3389/fenrg.2020.00017.

[40] Scarlat N, Fahl F, Dallemand J-F. Status and opportunities for energy recovery from municipal solid waste in Europe. Waste Biomass Valorization 2018;10(9):2425–44. https://doi.org/10.1007/s12649-018-0297-7.

[41] Soares Chinen A, Morgan JC, Omell B, Bhattacharyya D, Tong C, Miller DC. Development of a rigorous modeling framework for solvent-based CO_2 Capture. 1. Hydraulic and mass transfer models and their uncertainty quantification. Ind Eng Chem Res 2018;57(31):10448–63. https://doi.org/10.1021/acs.iecr.8b01471.

[42] Strahan, D. Net-Zero and Resource Efficiency by 2050, The Birmingham Policy Commission. 2020.

[43] Varme FO. OSLO_WTE_CCS_FEED-Study-Report-DG3_redacted_version. *Project CCS Carbon Capture Oslo*. 2021.

[44] Wienchol P, Szlęk A, Ditaranto M. Waste-to-energy technology integrated with carbon capture – Challenges and opportunities. Energy 2020;198. https://doi.org/10.1016/j.energy.2020.117352.

[45] Yoro KO, Daramola MO. CO_2 emission sources, greenhouse gases, and the global warming effect. In *Advances in Carbon Capture* (pp. 3-28). 2020.

[46] Zafar S. Trends in Waste-to-Energy Industry, BioEnergy Consult (available at: https://www.bioenergyconsult.com/trends-in-waste-to-energy-industry/) (Accessed: March 2022). 2022.

[47] Zanco SE, Pérez-Calvo J-F, Gasós A, Cordiano B, Becattini V, Mazzotti M. Postcombustion CO_2 capture: a comparative techno-economic assessment of three technologies using a solvent, an adsorbent, and a membrane. ACS Engineering Au 2021;1(1):50–72. https://doi.org/10.1021/acsengineeringau.1c00002.

[48] Zhang K, Liu Z, Li Y, Li Q, Zhang J, Liu H. The improved CO_2 capture system with heat recovery based on absorption heat transformer and flash evaporator. Appl Therm Eng 2014;62(2):500–6. https://doi.org/10.1016/j.applthermaleng.2013.10.007.